

RVE MODELLING OF DEFORMATION AND FAILURE BEHAVIOUR OF CLOSED CELL RIGID POLYMER FOAMS

Ralf Schlimper¹, Irene Vecchio², Katja Schladitz² and Ralf Schaeuble¹

¹Fraunhofer Institute for Mechanics of Materials IWM
Walter-Huelse-Str. 1, 06120 Halle, Germany

Email: ralf.schlimper@iwmh.fraunhofer.de, web page: <http://www.iwm.fraunhofer.de>

²Fraunhofer Institute for Industrial Mathematics ITWM
Fraunhofer-Platz 1, 67663 Kaiserslautern, Germany

Email: irene.vecchio@itwm.fraunhofer.de, web page: <http://www.itwm.fraunhofer.de>

Keywords: Finite Element Analysis, in situ testing, PMI foam, X-ray computed tomography

ABSTRACT

Closed cell rigid polymer foams are used as light core material in high loadable lightweight sandwich structures. Their mechanical behaviour depends on both the mechanical properties of the constituent solid polymer and the cellular structure on the mesoscopic scale which has therefore to be taken into account for the mechanical characterization of foam materials. This paper deals with the investigation of the deformation and failure behaviour of closed cell rigid polymer foams via numerical representative volume element (RVE) modelling approach. For this purpose the cellular structure of the foam was modelled by a 3d random Laguerre tessellation which was adapted to the real cellular structure of a closed cell Polymethacrylimide (PMI) foam in terms of morphological properties (e.g. cell size distribution) obtained from X-Ray computed tomography (X-Ray CT) data and subsequent 3d image analysis. In addition to the effective linear elastic material properties the strength of the foam model was calculated via finite element analysis (FEA) and consideration of nonlinear failure modes of the cellular structure. Parametric studies revealed the correlation between structural parameters (e.g. foam density, material content in the cell walls etc.) and the effective mechanical properties of the foam. Evaluation of the numerical results was done by standard mechanical testing of foam specimens on the one hand and X-Ray CT in situ deformation experiments with stepwise loading and scanning of foam specimens in a deformed state on the other hand. Both showed the potential of mesoscopic foam modelling with realistic consideration of the cellular structure as well as load case dependent deformation and failure mechanisms for exact prediction of material properties of closed cell foams.

1 INTRODUCTION

Closed cell rigid polymer foams are used as light core material in high loadable lightweight composite sandwich structures, e.g. in wind turbine blades and aircraft structures [1]. Their complex mechanical behaviour depends on both: the mechanical properties of the constituent solid polymer and the cellular structure on the mesoscopic scale. Latter causes a different mechanical behaviour depending on the load case e.g. compression or tension. Whereas the stress-strain diagram under compression load shows a distinctive stress-plateau due to subsequent layer-wise collapsing of the cell structure the foam fails comparatively brittle under tension load. First unit cell models for the mechanism based analysis of the deformation and failure behaviour were developed in the 1950/60ies [2, 3]. The famous cubic unite cell by Gibson and Ashby [4] idealizes the foam structure as a cubic arrangement of struts and plates. A further geometry which is commonly used for unite cell models of foam structures is the tetrakaidecahedral [5, 6]. Beside this unite cell models which were analysed analytically in most cases with upcoming computational power also multi cell models which represent a so called representative volume element (RVE) of the cellular foam structure were considered. Due

to their complex geometry they can only be solved numerically. Irregular cell structures similar to real foam structures can be modelled by the random Voronoi algorithm [7, 8, 9].

The objective of this paper is the modelling of the deformation and failure behaviour of a closed cell rigid foam made of Polymethacrylimide (PMI) via finite element analysis of an RVE model. The geometric model was built via a random Laguerre tessellation which allows to control the cell size distribution and to adapt it to the real cell structure in contrast to the Voronoi tessellation [10, 11, 15]. Thus the cell structure of the real foam is a necessary input for the modelling algorithm and was therefor analysed via X-ray computed tomography and subsequent quantitative 3d image analysis. The numerical results were evaluated via mechanical testing in standard compression, tension and shear tests. Furthermore the mechanical behaviour on the mesoscopic scale was investigated via in situ X-ray CT testing with stepwise loading and scanning of a foam specimen.

2 MATERIAL AND METHODS

2.1 PMI foam

Closed cell rigid polymer foams made of Polymethacrylimide (PMI) exhibit very good mechanical properties and dimensional stability under heat [12] compared to other polymer foams. Thus they are an appropriate core material in high loadable lightweight sandwich structures. Their nearly 100 percent closed cell structure consists of polyhedral cells with very thin planar cell walls and less material concentration in the struts (see figure 1 right). The investigations were done on foam grade ROHACELL® 71 RIST produced by the company Evonik Industries AG, Germany. The table in figure 1 gives an overview of its properties.

Density	kg/m ³	75,0
Young's modulus	MPa	105,0
Tensile strength	MPa	2,2
Strain at break	%	3,0
Compression strength	MPa	1,7

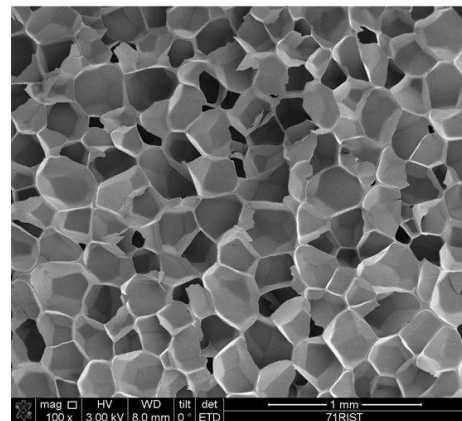


Figure 1: Material data of ROHACELL® 71 RIST [13] (left); SEM image of ROHACELL® 71 RIST (right)

2.2 RVE model of the cell structure

Stochastic geometry is used to model complex material structures on the mesoscopic scale. The random Laguerre tessellation which is a weighted generalization of the famous Voronoi tessellation is well suited for modelling of cellular structures with planar cell walls. For modelling the cell structure of a closed cell PMI foam, which is comparatively regular, the Laguerre tessellation is generated by a random closed packing of spheres. The cell size distribution of the cell model can be controlled effectively by the distribution of the sphere volumes. By choosing gamma or lognormal distributed sphere volumes the generated cell structure will be determined by the two parameters: 1) density of the sphere packing and 2) coefficient of variation of the sphere size distribution. However these parameters can't be determined directly from the morphological properties of the real foam structure measured in 3d image data taken by X-ray-CT. Rather a distance measure from the mean value and the coefficient of variation of the cell volume, the surface area, the mean width and the number of neighbor cells is calculated. The cell model will then be adapted to the real cellular structure by minimizing the distance measure between the model and the real structure within an iterative

procedure. Once the model parameters were identified they can be used to generate an arbitrary number of random model realizations with arbitrary size (number of cells). The thicknesses of cell walls and struts were applied within the next modelling step: generation of the finite element (FE) model. Further properties (e.g. angles between edges and faces) have less influence to the model adaption [17].

2.3 FEA of the RVE model

The mechanical behaviour of representative volume element models (RVE) of cellular materials can due to their complexity only be analyzed numerically, e.g. via finite element method FEM. It allows both calculation of the linear properties for small deformations and the typical nonlinear behavior of foams under static loads, e.g. for prediction of strengths. For that reason the components of the RVE model, cell walls and struts, were meshed with finite shell and beam elements which represent their mechanical behavior in an appropriate manner. The thickness of the beam (circular cross section) and shell elements was set according to the relative density of the foam which represents the volume fraction of the solid material within the volume of the whole RVE model (see equation 1). The thicknesses of cell walls t_w and struts t_s were assumed to be constant throughout the whole model:

$$R = \frac{\sum V_W + \sum V_S}{V_{RVE}} = \frac{t_w \sum A_W + 0,25 \cdot \pi t_s^2 \sum L_S}{V_{RVE}} \quad (1)$$

With V_W and V_S the volumes of cell walls and struts, further V_{RVE} the volume of the RVE model. From the density of the foam (75 kg/m³) and PMI bulk material (1200 kg/m³) the relative density of PMI foam ROHACELL® 71 RIST results: $R=0,0625$. The content of solid material in the struts is described by the parameter ϕ :

$$\phi = \frac{\sum V_S}{\sum V_S + \sum V_W} \quad (2)$$

The solid polymeric material was modelled with a simple isotropic bilinear elastic-plastic material model. The material data was partly taken from literature and partly determined via material testing: Youngs modulus $E_S=6480$ MPa and POISSON ratio $\nu_S=0,3$ from [16]; tangent modulus $E_{St}=150$ MPa and yield stress $\sigma_{Sp}=130$ MPa determined via tension tests of the PMI bulk material. The nonlinear calculations of the load cases uniaxial compression, tension and shear were run in ANSYS 14.5. The loads were applied in terms of nodal displacements. To prevent edge effects all nodes on the border of the geometrically periodic model were coupled via periodic boundary conditions.

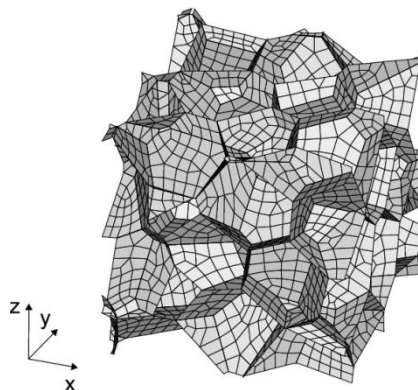


Figure 2: Meshed RVE model of the foam structure

2.4 X-ray computed tomography in situ testing

For the in situ X-Ray CT experiments a special test rig was built and integrated in a GE Phoenix nanome|x 180 NF X-Ray device (see figure 3). The test rig consists of a metal frame, the drive

mechanism for loading the specimen and the drive mechanism for rotating the specimen for the CT scan. It accounts for the low X-Ray absorption of foam specimens by prevention of any additional material in the X-Ray beam. The apparatus enables both tension and compression loading and is equipped with a 2.5 kN load cell. The cross head displacement is given by the number of steps driven by the loading drive mechanism.

An in situ compression test of a cylindrical foam specimen (diameter 11 mm, height 10 mm) was performed by stepwise loading and CT scanning of the loaded specimen. The load steps were applied in terms of fixed displacement steps according to 0.5 % nominal strain (given by the cross head displacement). The CT scan was performed ca. 10 minutes after the displacement step was reached to prevent uncertainties caused by relaxation of the specimen. The magnification was set to 16.7 which leads to a voxel size of 24 μm and enables the visualization of the complete specimen cross section. 23 load steps respective CT scans were applied to the specimen up to a nominal strain of 27 %. For each CT scan 1000 projections were recorded, which takes ca. 48 minutes.

A quasi static test was performed with the test rig and the same specimen geometry but without interruption and CT scanning for comparison of the load displacement curve.

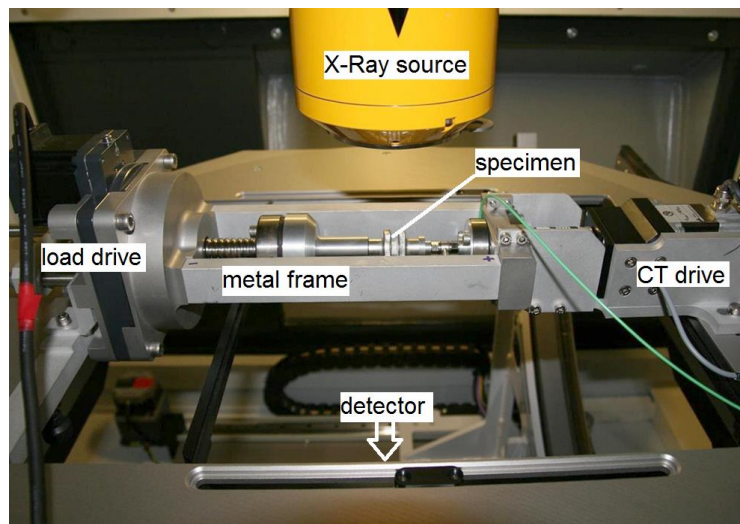


Figure 3: Testing device for in situ X-Ray CT

3 RESULTS

3.1 RVE model

In a first step the above mentioned morphological parameters of the real cellular structure of PMI foam ROHACELL® 71 RIST were determined from 3d images taken via X-ray computed tomography (see table 1). For the adaption of the random Laguerre tessellation its constituent parameters (density of sphere packing and variance of the sphere size distribution) were calculated in the subsequent step. Figure 4 (left) shows a 3d image data set of one scanned PMI foam specimen and one adapted model realization (Laguerre tessellation). The quality of the model adjustment can be evaluated by comparing the morphological characteristics of the model and the real cellular structure, e.g. the distribution of cell volumes (see figure 4 right).

	3d image data		Laguerre tessellation	
	mean value	CV	mean value	CV
cell volume in mm ³	0.013	0.64	0.010	0.71
cell width in mm	0.315	0.20	0.317	0.21
surface in mm ²	0.302	0.41	0.205	0.44
no. of neighbours	14.090	0.26	13.700	0.31

Table 1: Morphological parameters of the PMI foam ROHACELL® 71 RIST from 3d image analysis in comparison with the parameters of the adapted Laguerre tessellation

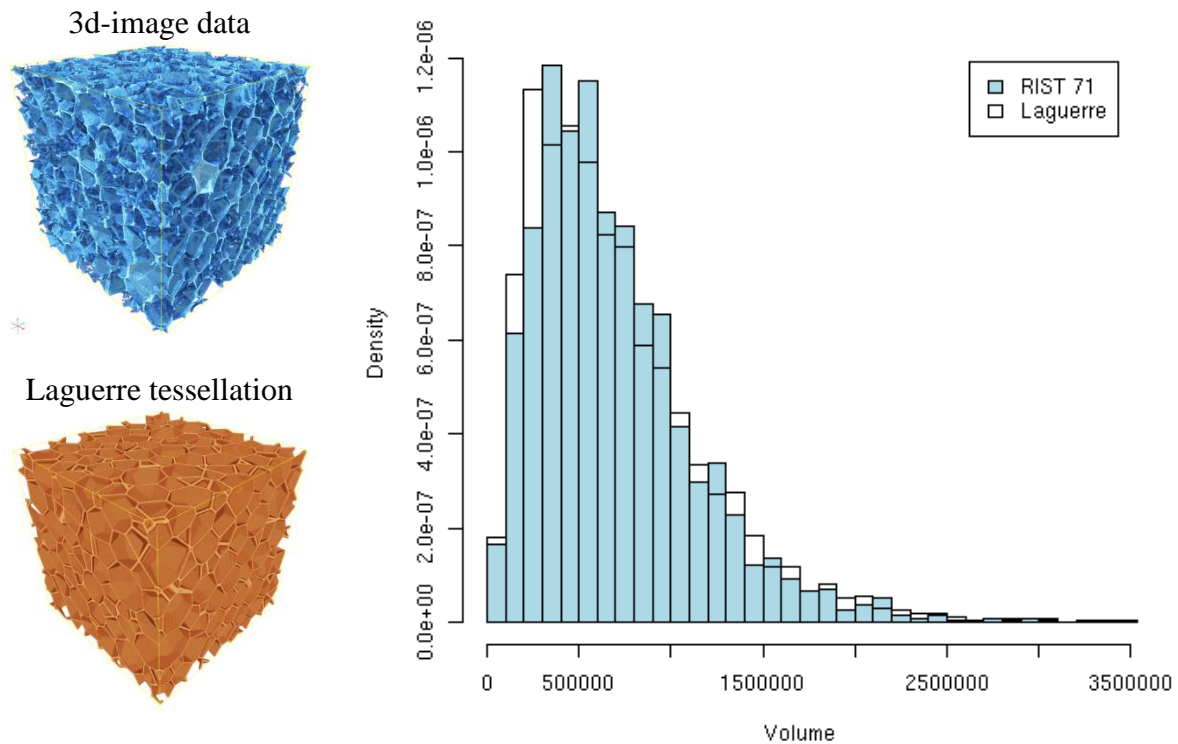


Figure 4: Left: Visualization of the 3d image data and the adapted 3d Laguerre tessellation (left); right: histogram of cell volumes from 3d image analysis (light blue) and the adapted Laguerre tessellation (white)

3.2 Elastic properties of the foam

The elastic properties in terms of the complete stiffness matrix assuming a general anisotropic linear elastic material behaviour was calculated from linear finite element calculations of the RVE model which was adapted to PMI foam ROHACELL® 71 RIST. Therefore several load cases were applied to the model. If the model contains a sufficient number of cells the mechanical response of the model is nearly isotropic. In that case the stiffness matrix was reduced to the set of effective linear elastic material constants Young's modulus, shear modulus and POISSON's ratio. Within parametric studies a number of 125 cells was identified to be sufficiently representative for the investigated foam structure. Then the variance of the results calculated from various random realizations of the RVE model was minimal.

Within parametric studies the influences of a) content of solid material in the struts ϕ and b) the relative density R to the effective elastic material constants of the foam were investigated. Hence both

calculated modulus decrease with increasing ϕ but under different rates. Thus the POISSONs ratio increases with ϕ (see figure 5 left). Due to the fact that the content of solid material in the struts could not be determined from 3d image data (for resolution reasons) it was calculated inversely by adjusting the model to the Youngs modulus of 105 MPa which is given in the material data sheet of ROHACELL® 71 RIST [13]. This is the case for $\phi=0.32$. The elastic properties of the according RVE model are shown in figure 5 (right) for density variance of $\pm 20\%$. The correlation between density and the elastic constants is nearly linear.

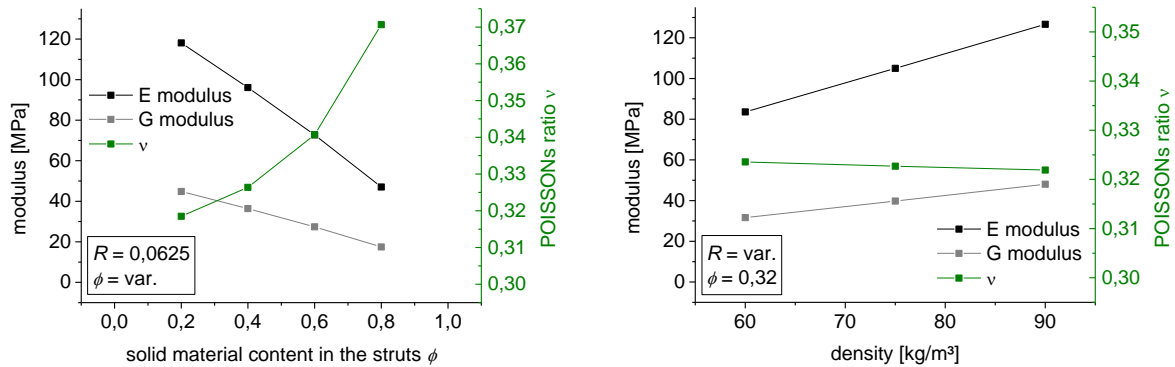


Figure 5: Calculated modulus and POISSONs ratio for PMI foam ROHACELL® 71 RIST vs. solid material content in the struts (left) and foam density (right)

3.3 Deformation and failure behaviour observed via X-Ray CT in situ testing

Load-displacement curve

The load-displacement curve recorded during the in situ compression test is shown on figure 6. On every applied load step the load increases quite linearly and drops down after the cross head stops due to the relaxation of the foam specimen. On load-time-plots it becomes obvious that the main part of the relaxation happens within the first 10 minutes after the load was applied. In the first load step a nominal strain of 1 % was applied, afterwards load was applied in steps of 0.5 % nominal strain. After the 5th load step which thus corresponds to 3 % nominal strain load did not increase further but remains on a nearly constant level. In the following load steps only the load drop caused by relaxation is compensated during the loading step. The relaxation increases with increasing load level due to the nonlinear viscoelastic behaviour of the PMI foam as described in [18]. Due to the scanning time of 48 minutes the complete experiment runs 3 days and was interrupted over night after load step 7 and 14, where the load drop due to the relaxation is significantly larger. Within the last load steps where nominal strains of 5 and 10 % were applied the crushing failure of the cell structure becomes obvious even in the load displacement curve by formation of a load plateau. The collapse of single foam cells starts on even earlier load steps, which was observed in the image data.

The second load displacement curve shown in figure 6 was recorded on a continuous quasi static compression test in a standard testing machine and the same specimen geometry. It is in good accordance to the one recorded during the in situ test. Whereas the slopes of the curves are nearly identical the strength measured during in situ test is ca. 8 % lower but still fits quite well to the compression strength given in the material data sheet (see Table 2). However the Young's modulus calculated from the load displacement data is ca. 25 % lower than the one given in Table 2 which is due to the overestimation of the strain calculated from the cross head displacement.

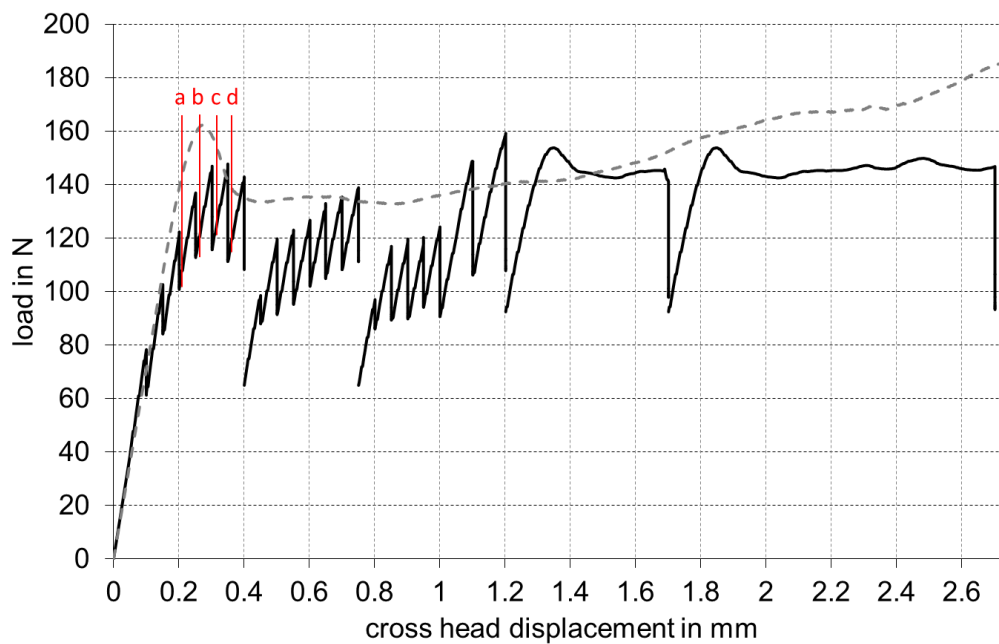


Figure 6: Recorded load displacement curve of in situ compression test (black lines) and continuous static compression test (dashed grey line)

CT images

The CT images taken between the load steps were analyzed qualitatively in terms of a single slice near the center of the specimen which was tracked over all load steps. A sequence of such slice images is given in figure 7. By visual inspection of the image stacks the cell which initially collapses was detected (sections on the right of figure 7). The two upper cell walls of this cell are oriented at an angle of $\pm 45^\circ$ to the vertical loading direction. On 2 % nominal strain S-shaped buckling of one of them occurs while the adjacent cells remain unaffected (figure 7a). On the next load step the other one starts buckling in the same manner (figure 7b). One load step further a band of collapsed cells can be observed on the left side of the specimen (figure 7c). In the following load step it covers the whole cross section but spans on different height levels (see figure 7d). With further progress of the test this band propagates through the whole specimen height. The foam cells outside this crush band remain nearly unaffected. Regarding the recorded load displacement curve it becomes obvious that the maximum load is reached when the crush band forms. The elastic deformation of cell walls and struts could hardly be detected because it is in the same order of magnitude with the voxel size and could therefore not properly be resolved. Cell reconstruction analysis as described above reveals that the volume of the initial collapsing cell is three times above the average cell volume and its cell walls are therefore prone to buckling.

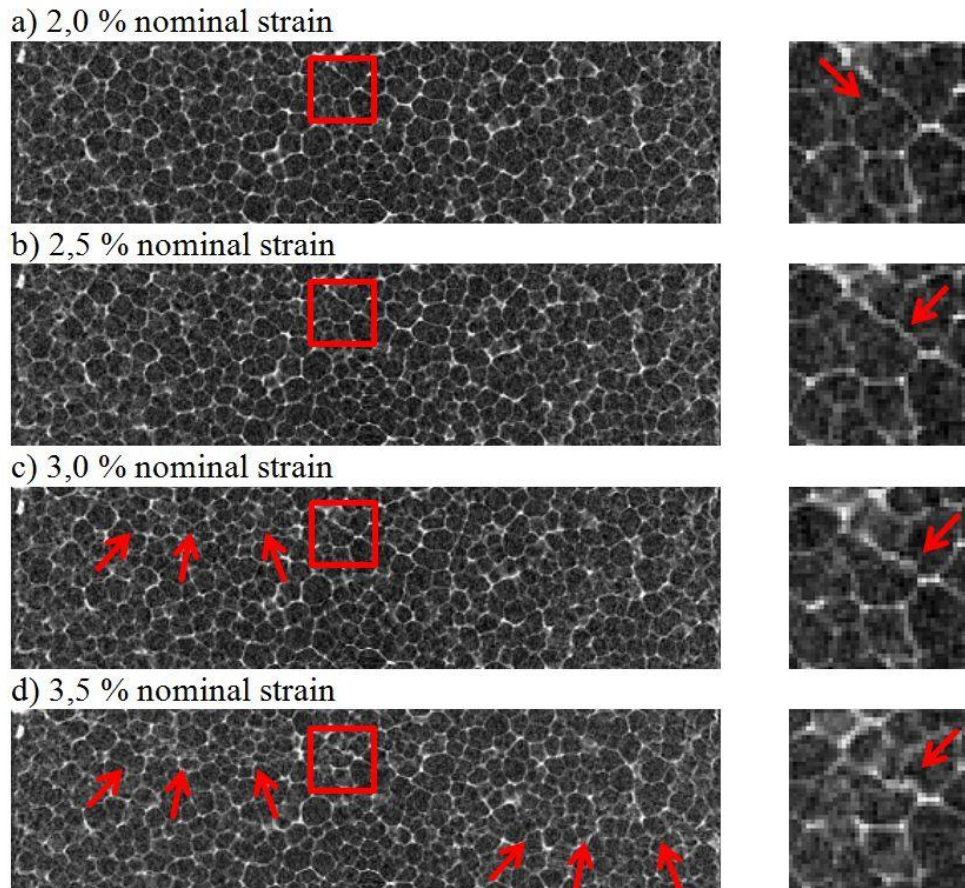


Figure 7: Slices of CT images recorded during in situ compression test (loading direction vertical) on different load levels, zoom image of initially collapsed cell

3.4 Nonlinear FEA

Nonlinear stress strain behaviour

The nonlinear stress-strain curves calculated from an adapted RVE model (continuous line in figure 8) are qualitatively in good accordance to the ones measured at the real PMI foam (dashed lines in figure 8). The differences between testing and modelling in the initial stiffness under tension and compression are due to the experimental test set up. The specific boundary conditions during the tests which were run on cubic specimens lead to higher apparent stiffness' which were not representative for the material behaviour. The elastic constants calculated from the initial slopes of the calculated curves were in good accordance to the material data sheet given by the manufacturer. The strengths were determined in terms of characteristic points in the calculated stress-strain curves, comparable to the analysis of experimental data from tensile, compression and shear tests. Hence a limit stress corresponding to 0,2% plastic strain was determined in the tensile load case (dots in figure 8). For the compression and shear load case the maximum stress in the calculated strain interval was defined to be the limit stress. Table 2 gives an overview of the calculated properties and compares them to the data given in the material data sheet.

		FEA	Data sheet
Youngs modulus	MPa	104	105
shear modulus	MPa	40	42
tensile strength	MPa	2,3	2,2
compression strength	MPa	1,8	1,7
shear strength	MPa	1,3	1,3

Table 2: Comparison between calculated mechanical properties of PMI foam ROHACELL® 71 RIST and data given in the material data sheet by the manufacturer [13]

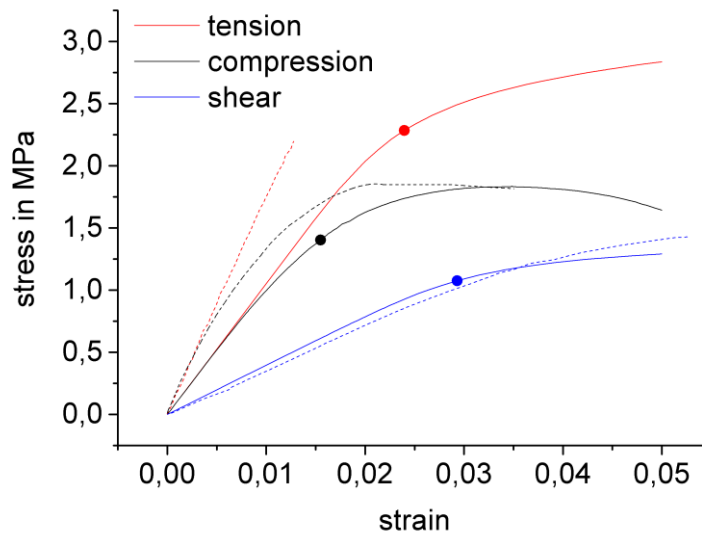


Figure 8: Calculated stress strain curves for PMI foam ROHACELL® 71 RIST (continuous lines) with 0.2% plastic strain limit (marked dots) in comparison to experimental curves (dashed lines)

Deformation and failure mechanisms

From the nonlinear finite element analysis of the RVE model the strains and stresses in struts and cell walls could be analyzed component wise which enables a deep investigation of deformation and failure modes of the cellular structure. By means of the calculated strain energies it was found that the initial linear elastic regime is dominated by axial deformation of the cell walls. Via accompanying eigenvalue calculation the occurrence of first instabilities was determined in the stress strain curves. Thus first cell wall buckling occurs in both compression and shear loading already at load levels < 20 % of the failure load and consequently can not be the sole reason for failure of the foam structure. Rather the collapse of cells is caused by the elastic-plastic material behaviour of the solid polymer material in the cell walls. Figure 9 shows a central section of the RVE model a) unloaded, b) under vertical compression load at 0,2% limit stress and c) at maximum stress. It becomes obvious that plastic yielding (red marked cell walls) occurs predominantly in regions where also cell wall buckling occurs. Both cell wall buckling and plastic yielding of the solid material are localized in one layer perpendicular to the vertical loading direction (highlighted by the dotted lines in figure 9c), which is the initial cell layer for the layer-wise collapse of the cell structure, as it was already observed during the X-ray in situ compression experiments. Analogue to the compression load case, which was described here, the other load cases (tension and shear) were analyzed in a similar manner to get a detailed knowledge of the deformation and failure behaviour of polymeric cellular structures.

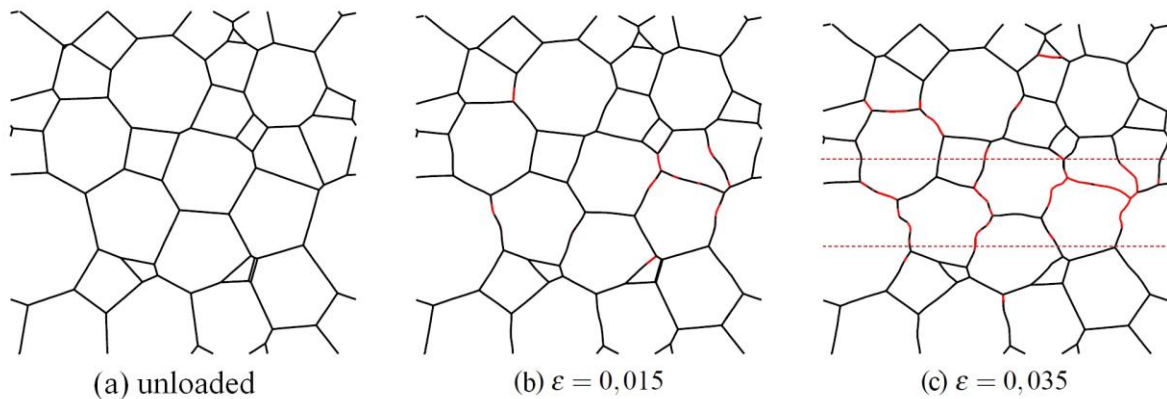


Figure 9: Central section through the RVE model under vertical compression load, cell walls where plastic yielding of the solid material occurs are marked in red colour

4 CONCLUSIONS

The deformation and failure behaviour of a closed cell PMI foam was investigated in terms of a RVE modelling approach, numerical analysis and X-Ray CT in situ testing. The in situ compression test of a foam specimen which was performed by application of a special test rig in the X-Ray CT device enhances the knowledge about the characteristic mechanisms on mesoscopic scale involved in deformation and failure behaviour of rigid polymer foams. It reveals that local buckling of cell walls occurs already in the macroscopic linear elastic region of the load displacement curve and that the maximum load is reached when a complete layer of cells collapses. The cell which initially collapses was found to be three times larger than the average. Based on these findings the cellular structure was modelled by a random Laguerre tessellation which was adapted to the real structure in terms of the cell size distribution to get a deeper knowledge about the correlation between the cellular structure and the mechanical behaviour and the influence of morphological parameters. The appropriate applicability of the random Laguerre tessellation for modelling closed cell PMI foams was proved on both the accordance of morphological/geometrical parameters between the model and the real structure and the accordance between the numerical analysis and the experimental characterization of the mechanical behaviour of the foam. Thus the RVE modelling approach enables not only the prediction of linear elastic constants but also strengths of the foam and the assessment of influences of morphological and physical parameters, like local variances of densities which can typically occur and the distribution of solid material between cell walls and struts.

ACKNOWLEDGEMENTS

This work was partially funded by the Federal Ministry of Economics and Technology in the AiF program by the IGF project 16912BG/1. The authors wish to acknowledge for this support.

REFERENCES

- [1] Zahlen, P.C. ; Rinker, M. ; Heim, C.: Advanced manufacturing of large, complex foam core sandwich panels. In: Ferreira, A.J.M (Ed.): *Proceedings of 8th International Conference on Sandwich Structures*. Porto, 2008, pp. 606–623
- [2] Gent, A. N. ; Thomas, A. G.: The deformation of foamed elastic materials. In: *Journal of Applied Polymer Science* **1**, 1959, pp. 107–113
- [3] Ko, W.L.: Deformations of foamed elastomers. In: *Journal of Cellular Plastics* **1**, 1965, pp. 45–50
- [4] Gibson, L. J. ; Ashby, M. F.: Cellular solids - Structure and properties. Cambridge : *Cambridge University Press*, 1988
- [5] Dement'ev, A.G. ; Tarakanov, O.G.: Effect of cellular structure on the mechanical properties of plastic foams. In: *Polymer Mechanics* **6**, 1970, pp. 519–525

- [6] Zhu, H. X. ; Knott, J. F. ; Mills, N. J.: Analysis of the elastic properties of open-cell foams with tetrakaidecahedral cells. In: *Journal of the Mechanics and Physics of Solids* **45**, 1997, pp. 319–343
- [7] Shulmeister, V.: Modelling of the Mechanical Properties of Low-Density Foams, TU Delft, Diss., 1998
- [8] Ribeiro-Ayeh, S.: Finite Element Modeling of the Mechanics of Solid Foam Materials, *School of Engineering Sciences, Kungliga Tekniska Högskolan (KTH)*, Diss., 2005
- [9] Köll, J., Hallström, S.: Generation of stochastic foam models for numerical analysis. *Journal of Cellular Plastics*, **50** (1), 2014, pp. 37-54
- [10] Lautensack, C.: Random Laguerre tessellations, *Fakultät für Mathematik der Universität Karlsruhe (TH)*, Diss., 2007
- [11] Ohser, J. ; Schladitz, K.: 3D Images of Material Structures, Processing and Analysis. *Weinheim : Wiley-VCH Verlag*, 2009
- [12] Domininghaus, H. ; Eyerer, P. (Ed.) ; Elsner, P. (Ed.) ; Hirth, T. (Ed.): *Kunststoffe: Eigenschaften und Anwendungen. Heidelberg : Springer Verlag*, 2005
- [13] Evonik Industries AG Performance Polymers, Material Data Sheet, downloaded from www.rohacell.com on April 2012
- [14] Seibert, H. F.: Applications for PMI foams in aerospace sandwich structures. In: *Reinforced Plastics* **50**, 2006, pp. 44 – 48
- [15] Lautensack, Fitting three-dimensional Laguerre tessellations to foam structures. *Journal of Applied Statistics*, **35**, 2008, pp.985-995
- [16] Chen, C. P. ; Anderson, W. B. ; Lakes, R. S.: Relating the properties of the foam to the properties of the solid from which it is made. In: *Cellular Polymers* **13**, 1994, pp. 16–32
- [17] Vecchio, I. ; Redenbach, C. ; Schladitz, K.: Angles in Laguerre tessellation models for solid foams. In: *Computational Materials Science* **83**, 2014, pp. 171-184
- [18] John, M.; Schlimper, R.; Rinker, M.; Wagner, T.; Roth, A.; Schäuble, R: Long-term durability of CFRP foam core sandwich structures *CEAS Aeronautical Journal*, Springer Wien, 2011, 2, pp. 213-221